

# APPO: Attention-guided Perception Policy Optimization for Video Reasoning

Henghui Du<sup>1,2,\*</sup>, Chang Zhou<sup>2,✉</sup>, Xi Chen<sup>2</sup>, Di Hu<sup>1,✉</sup>

<sup>1</sup>Gaoling School of Artificial Intelligence, Renmin University of China, Beijing, <sup>2</sup>AI Technology Center, Online Video Business Unit, Tencent PCG

\*Work done at Tencent PCG, ✉ Co-Corresponding author

arXiv:2602.23823v1 [cs.CV] 27 Feb 2026

## Abstract

Complex video reasoning, actually, relies excessively on fine-grained perception rather than on expert (*e.g.*, Ph.D, Science)-level reasoning. Through extensive empirical observation, we have recognized the critical impact of perception. In particular, when perception ability is almost fixed, enhancing reasoning from Qwen3-8B to OpenAI-o3 yields only 0.7% performance improvement. Conversely, even minimal change in perception model scale (from 7B to 32B) boosts performance by 1.4%, indicating enhancing perception, rather than reasoning, is more critical to improve performance. Therefore, exploring how to enhance perception ability through reasoning without the need for expensive fine-grained annotation information is worthwhile. To achieve this goal, we specially propose **APPO**, the **A**ttention-guided **P**erception **P**olicy **O**ptimization algorithm that leverages token-level dense rewards to improve model’s fine-grained perception. The core idea behind APPO is to optimize those tokens from different responses that primarily focus on the same crucial video frame (called *intra-group perception tokens*). Experimental results on diverse video benchmarks and models with different scales (3/7B) demonstrate APPO consistently outperforms GRPO and DAPO (0.5% ~ 4%). We hope our work provides a promising approach to effectively enhance model’s perception abilities through reasoning in a low-cost manner, serving diverse scenarios and demands.

**Email:** <sup>1</sup>{cserdu, dihu}@ruc.edu.cn, <sup>2</sup>{cserdu, chanzhou, jasonxchen}@tencent.com

**Project Page:** <https://gewu-lab.github.io/APPO>

**Code:** <https://github.com/GeWu-Lab/APPO>

**Date:** 2026-03-02

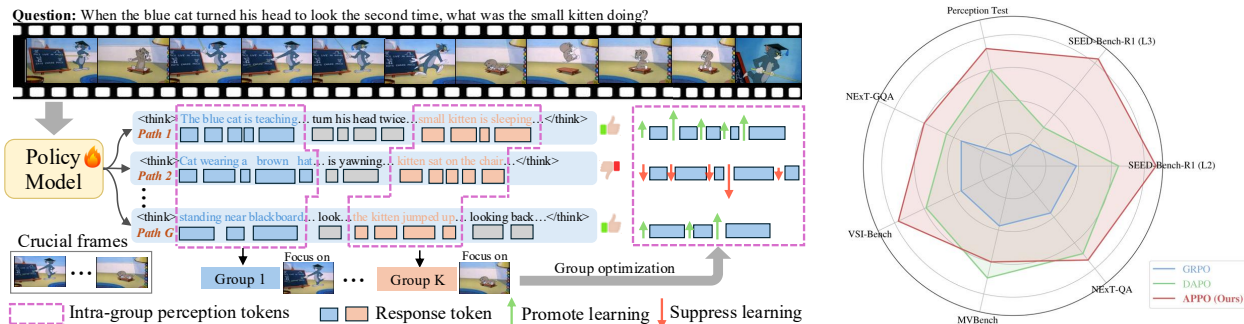


**Figure 1** We present **APPO**, the **A**ttention-guided **P**erception **P**olicy **O**ptimization algorithm that enhances model’s fine-grained perception ability through reasoning. The core idea behind APPO is to optimize those tokens from different responses that primarily focus on the same crucial video frames (called *intra-group perception tokens*), resulting in fine-grained token level reward signals. **Left:** The illustration of APPO algorithm. The intra-group perception tokens are defined as those tokens from different responses that primarily focus on the same crucial video frame. The perception tokens within each group are optimized with different learning intensities. **Right:** Experimental results on multiple video benchmarks demonstrate APPO achieves overall performance improvement compared with GRPO and DAPO.

# 1 Introduction

Reinforcement Learning with Verifiable Rewards (RLVR) has proven to be a highly effective strategy for endowing Large Language Models (LLMs) with powerful reasoning abilities to solve complex tasks [1, 2]. DeepSeek-R1 [2] employs verifiable signals, such as structured thinking formats and final answer accuracy to optimize models through Group Relative Policy Optimization (GRPO) algorithm. Subsequent works, such as DAPO [3] and GSPO [4] *etc.*, have consistently achieved superior performance improvements compared to Supervised Fine-Tuning (SFT). Motivated by this success, a growing body of works [5–8] have explored applying RLVR to video scenarios, in hopes of improving the video reasoning abilities of MLLMs. By specially designing sparse outcome reward signals for different types of tasks, such as IoU of bounding box and timestamps, *etc.*, they have yielded remarkable success, particularly in terms of generalization ability.

Despite significant progress in most prior efforts, they have primarily focused on improving data quality [14, 15] or rewards design [16, 17]. It should be noted that different from text-based tasks, complex video reasoning involves *fine-grained perception* and multi-step reasoning, both of which are essential and extremely important. Intuitively, perception is the foundation and premise for reasoning. For example, as shown in Fig. 1, if the model fails to notice the critical behavior of the small kitten sleeping, or confuses the sequence of blue cat turning its head twice, it would be very difficult to reason out the correct answer. While it might be solved based on contextual information, such as the small kitten yawning and stretching, this requires stronger reasoning and self-correction capabilities, which increases the burden on the model. Therefore, this situation presents us two fundamental research question: **(1) For video reasoning, what is the key to improve model’s performance, enhancing perception or reasoning?** **(2) If perception, how to design a perception optimization strategy to effectively enhance fine-grained perception without relying on expensive fine-grained annotation or additional reward models?**

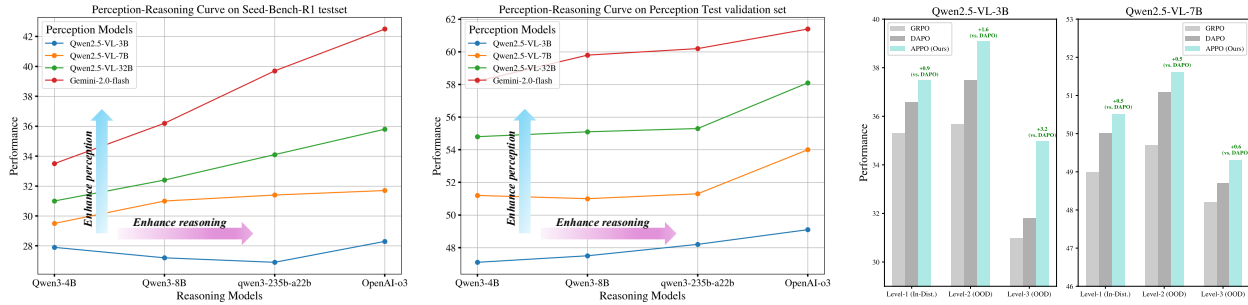
To investigate the first question, we employ an innovative divide-and-conquer strategy to quantify the impact of perception *vs.* reasoning on overall performance. Specifically, we modularize the capabilities of perception and reasoning, leveraging four perception models and four reasoning models with progressively enhanced abilities. By controlling variables, they are cross-combined to form a grid-based evaluation. As a result, the **Perception-Reasoning curves** on two benchmarks are shown in Fig. 2. It can be easily observed that: (1) when one capability (either perception or reasoning) is fixed, enhancing the other leads to

an overall trend of improved performance; (2) enhancing perception ability results in a more remarkable improvement than enhancing reasoning. For example, on SEED-Bench-R1 benchmark, when the perception model is fixed as Qwen2.5-VL-7B, changing the reasoning model from Qwen3-8B to OpenAI-o3 only results in 0.7% improvement; conversely, changing the perception model from Qwen2.5-VL-7B to Qwen-2.5-VL-32B, even this minimal change in model scale can enhance the performance of the Qwen3-8B model by 1.4%. This suggests that in complex video scenarios, enhancing perception ability, rather than reasoning, is more important to improve performance.

Building upon above observations, we specially propose **APPO**, the **Attention-guided Perception Policy Optimization** algorithm that enhances model’s fine-grained perception through reasoning. Indeed, existing popular RL methods struggle to effectively enhance model’s fine-grained perception capabilities, mainly because sparse outcome rewards fail to provide sufficient fine-grained guidance signals, and fine-grained perception annotations are costly. Therefore, to bridge these gaps, our APPO algorithm aims to establish fine-grained reward signals directly from sparse outcome rewards without relying on expensive annotation or additional reward models. To be specific, APPO algorithm primarily consists of two core steps: **1) Transform sparse outcome rewards into dense, frame-level guidance signals.** Those reasoning trajectories with higher rewards are used to identify potentially important frames. These frames are considered necessary to be focused on by paths with lower rewards. **2) Compute token-level fine-grained rewards for intra-group perception tokens.** Tokens from different paths that focus on the same frames (called *intra-group perception tokens*) are assigned to the same group. The discrepancy among these tokens is measured by  $KL$  divergence, prioritizing learning tokens from high-reward paths, while suppressing those from low-reward paths, resulting in the token-level fine-grained rewards. Experimental results on diverse video benchmarks and models with different scales demonstrate APPO consistently outperforms existing algorithms, such as GRPO and DAPO.

In summary, our contributions are as follows:

- Building upon divide-and-conquer strategy and extensive experiments, we quantify the impact of perception and reasoning on overall performance, and found that enhancing perception could yield more remarkable performance improvements compared to enhancing reasoning.
- To enhance model’s fine-grained perception ability during reasoning, we propose APPO algorithm that encourages model to prioritize learning of intra-



(a) SEED-Bench-R1 benchmark. (b) Perception Test benchmark. (c) Performance on SEED-Bench-R1.

**Figure 2** The **Perception-Reasoning curves** on SEED-Bench-R1 [9] and Perception-Test [10] benchmarks, quantifying the impact of perception vs. reasoning ability on overall performance. Each point in the curve represents the performance achieved by combining specific perception and reasoning ability. In particular, we first prompted four perception models with progressively enhanced abilities (including Qwen2.5-VL-3/7/32B [11] and Gemini-2.0-flash [12]) to describe video content in detail. Subsequently, the other four reasoning models with varying capabilities (including Qwen3-4/8B, Qwen3-235-A22B-thinking [13], and OpenAI-o3 [1]) were used to think and answer questions based on the descriptions provided by each perception model, respectively, yielding  $4 \times 4$  cross-combination results. (a) For SEED-Bench-R1 benchmark, we evaluate on  $2K$  Level-1 samples. (b) For Perception Test benchmark, we randomly select  $1K$  samples from different videos for evaluation. (c) The performance comparison of GRPO, DAPO and our APPO on SEED-Bench-R1 benchmark across different scales models, demonstrating the significant improvements brought by enhanced perception.

group perception tokens by leveraging token-level fine-grained rewards.

- Experimental results on diverse video benchmarks and models with different scales consistently demonstrate the effectiveness of APPO. Our work provides a promising approach to effectively enhance model’s perception abilities through reasoning in a low-cost manner, serving diverse scenarios and demands.

## 2 Related Works

### 2.1 Large Language Model Reasoning

Recent advances in Reinforcement Learning (RL) have significantly enhanced the reasoning capabilities of Large Language Models (LLMs) [1–4]. The GRPO (Group Relative Policy Optimization) proposed by DeepSeek-R1 [2] demonstrated that pure reinforcement learning can significantly enhance the robust reasoning capabilities of the model based on verifiable reward signals. To address several key issues faced by GRPO algorithm, such as entropy collapse, reward noise, and training instability, Qiying *et al.* [3] proposed the DAPO algorithm. substantially improves model’s reasoning capabilities by designing verifiable reward signals, including structured thought formats and final answer accuracy. The DAPO [3]. Further, Chujie *et al.* [4] introduced GSPO to resolve the stability challenges in the RL training of large Mixture-of-Experts (MoE) models. The design and optimization of these policy optimization algorithms are tailored for purely textual domains. Similarly, the APPO algorithm proposed in this work is specially designed for video reasoning tasks.

### 2.2 Video Reinforcement Fine-tuning

Inspired by the success of reinforcement learning in text-based tasks, many studies [5, 6, 8, 9, 16, 17] have applied the learning paradigm to vision tasks, achieving significant improvements. Time-R1 [16], Space-R [17] and Video-R1 [5] *etc.* design proprietary reward signals for specific types of tasks, such as bounding box and time IoU to enhance the temporal and spatial reasoning capabilities of models. To make the reasoning process of models more reliable, some studies [18–20] utilize the inherent grounding capabilities of models as a tool to select the necessary data from images or videos. While the learning paradigms used in text-based tasks have achieved decent results in these visual tasks, they fail to effectively enhance the model’s perceptual abilities, thus the performance of the model remains limited. Differently, our work starts from the perspective of video reasoning, experimentally observes and analyzes the importance of perception abilities, and specifically proposes optimization strategies to enhance model’s fine-grained perception capabilities during the reasoning process.

### 2.3 Perception-aware Reinforcement Learning

Recent works [21, 22] have also recognized the importance of perception. Visionary-R1 [21] and Perception-R1 [22] introduced additional rewards that either directly assess perception quality or require the model to explicitly perform captioning before reasoning. While promising, these strategies often impose a rigid separation between perception and reasoning, rather than enabling joint learning of both. They also rely on additional large neural-

based reward models, resulting in significant computational overhead and limitations imposed by the reward model’s capacity. Our APPO algorithm could jointly improve fine-grained perception and reasoning without relying on additional reward models.

### 3 Methodology

In this section, we first introduce post-training methods for reinforcement fine-tuning in subsection 3.1, such as GRPO. Then, we propose APPO, the Attention-guided Perception Policy Optimization algorithm that enhances fine-grained perception ability while reasoning.

#### 3.1 Preliminary

**Task Formulation.** Following a typical setting, a training sample  $x$  from dataset  $\mathcal{D}$  contains video input  $\mathcal{V} = \{I_i \in \mathbb{R}^{H \times W \times C}\}_{i=1}^T$ , where  $H, W, C$  represent the height, width and channels respectively,  $T$  is the number of video frames, question  $q$ , and ground truth answer  $a$ . We do not rely on any existing chain-of-thought data and initiate RL training directly without cold-start SFT.

**GRPO.** For an input sample  $x = \{\mathcal{V}, q, a\}$ , a group  $G$  candidate responses  $o = \{o_1, o_2, \dots, o_G\}$  are sampled from old policy model  $\pi_{\theta}^{\text{old}}$ . A simple rule-based verifier is used to compute reward scores  $\{r_1, r_2, \dots, r_G\}$  for these responses. To quantify the relative quality of each response, the rewards are standardized within the group:

$$A_i = \frac{r_i - \mu}{\sigma}, \quad \mu = \text{mean}(\{r_i\}), \quad \sigma = \text{std}(\{r_i\}), \quad (1)$$

where  $A_i$  is advantage calculated based on the relative reward within the group. Then the policy model  $\pi_{\theta}$  is optimized with the following objective (we omit the clip term for simplicity):

$$\mathcal{L}_{\text{GRPO}} = \mathbb{E}_{o \sim \pi_{\theta}^{\text{old}}} \left[ \frac{1}{N} r_{i,t}(\theta) \cdot A_i - \beta \cdot \text{KL}[\pi_{\theta} \parallel \pi_{\text{ref}}] \right], \quad (2)$$

$$\text{where } \frac{1}{N} = \frac{1}{G} \sum_{i=1}^G \frac{1}{|o_i|} \sum_{t=1}^{|o_i|}, \quad r_{i,t}(\theta) = \frac{\pi_{\theta}(o_{i,t}|q, o_{i < t})}{\pi_{\theta}^{\text{old}}(o_{i,t}|q, o_{i < t})}.$$

#### 3.2 Attention-guided Perception Policy Optimization (APPO)

To enhance the model’s fine-grained perception capabilities during reasoning, we propose **APPO**, the Attention-guided Perception Policy Optimization algorithm. The key idea behind APPO is to encourage the model to prioritize learning those intra-group tokens that focus on the same potentially important frame (intra-group perception tokens). Fig. 3 shows an illustrative overview of the

algorithm, which primarily consists of two core steps: attention-guided frame selection and intra-group perception tokens re-weighting. Next, we formally introduce these two key components as follows.

**Attention-guided Frame Selection.** Essentially, the most intrinsic representation of model’s perception is the attention scores on video frames. Those responses with higher rewards are more likely to focus on the correct video frames. Conversely, those with lower rewards are likely to suffer from missing or not focusing on these frames. Therefore, this discrepancy can be used to identify potentially important video frames, thus transforming sparse outcome rewards into dense, frame-level guidance signals.

To be specific, as shown in right part of Fig. 3, the  $G$  responses are first divided into two sets based on the reward scores, namely:

$$S_1 = \{o_i \mid r_i \geq \tau\}, \quad S_2 = \{o_i \mid r_i < \tau\}, \quad (3)$$

where  $\tau$  is a reward threshold. Then we track the attention weights from response tokens to visual tokens. For the  $h$ -th layer, let  $a_{jv}^{(h)}$  represents the attention weight from the  $j$ -th response token to the  $v$ -th visual token. The average attention weight from the  $j$ -th response token to the  $t$ -th frame  $f_t$  is given by:

$$\text{Attn}(j, f_t) = \frac{1}{\sum_h \cdot |f_t|} \sum_h \sum_{v \in f_t} a_{jv}^{(h)}, \quad (4)$$

where  $|f_t|$  represents the visual token numbers of  $f_t$ . Then the attention weights of response  $o_i$  towards the  $t$ -th frame  $\text{Attn}(o_i, f_t)$  is calculated by:

$$\phi(i) = \text{TopK}_j(\text{Attn}(o_{i,j}, f_t), K_1), \quad (5)$$

$$\text{Attn}(o_i, f_t) = \frac{1}{K_1} \sum_{j \in \phi(i)} \text{Attn}(o_{i,j}, f_t), \quad (6)$$

where  $o_{i,j}$  represents the  $j$ -th token in response  $o_i$ ,  $\phi(i)$  is the set of token indices in  $o_i$ , corresponding to  $K_1$  tokens with the highest attention weights to  $f_t$  and  $|\phi(i)| = K_1$ . Following that, the video frames that primarily focused on by response  $o_i$  can be denoted as:

$$\psi(i) = \text{TopK}_t(\text{Attn}(o_i, f_t), K_2), \quad (7)$$

where  $\psi(i)$  is a set of frame indices, corresponding to  $K_2$  video frames that are most focused on by  $o_i$  and  $|\psi(i)| = K_2$ . To obtain a more comprehensive set of important video frames, we take the union of  $\psi(i)$  within the sets  $S_1$  and  $S_2$ , respectively:

$$\psi^{S_1} = \bigcup_{o_i \in S_1} \psi(i), \quad \psi^{S_2} = \bigcup_{o_i \in S_2} \psi(i), \quad (8)$$

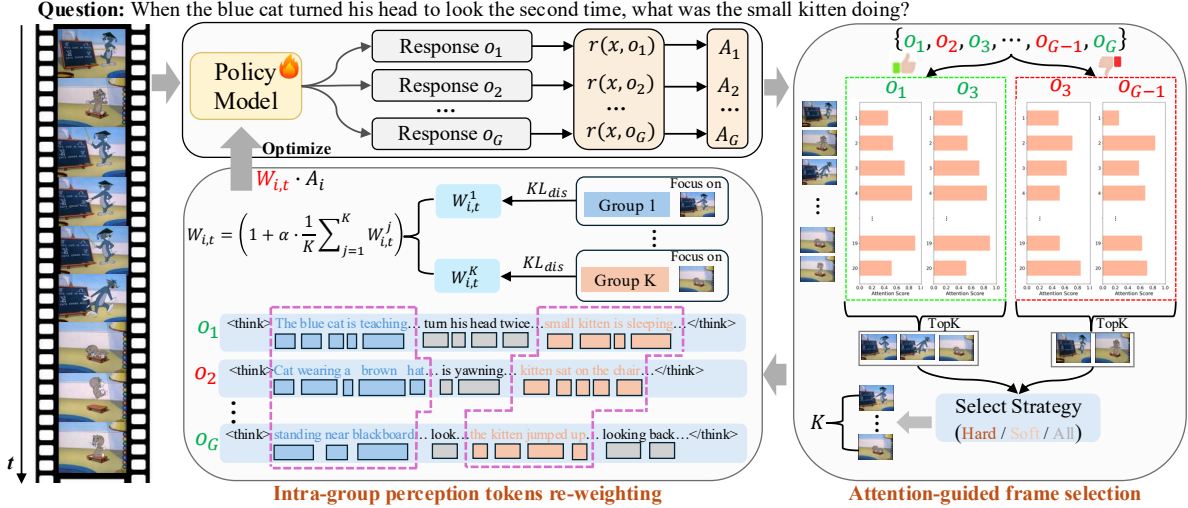


**Figure 3** The overview of APPO algorithm, which primarily consists of two core steps: attention-guided frame selection and intra-group perception tokens re-weighting. Firstly, a group of  $G$  responses are divided into two sets based on the reward scores, and the final target frames are selected from these two sets based on attention weights. Building upon these frames, those tokens from different responses focusing on the same frame are assigned into a group and optimized with token-level weights.

where  $\psi^{S_1}$  and  $\psi^{S_2}$  are considered the video frames most focused on by high-reward and low-reward responses.

The final selected frames  $\psi'$  are selected from these two sets through three available strategies: 1) Hard. Strictly select target frames based on the difference between  $\psi^{S_1}$  and  $\psi^{S_2}$ , that is:  $\psi' = \psi^{S_1} \setminus \psi^{S_2}$ ; 2) Soft. To comprehensively promote the learning of frame-level fine-grained perception, use the  $\psi^{S_1}$  as the target frames:  $\psi' = \psi^{S_1}$ ; 3) All. Consider all frames focused on by both sets as target frames, namely  $\psi' = \psi^{S_1} \cup \psi^{S_2}$ . Ultimately, these selected frames  $\psi'$  are used to optimize those intra-group perception tokens, as described in the following.

**Intra-group Perception Tokens Re-weighting.** For each frame in  $\psi'$ , there will be several tokens from  $G$  responses focusing on it, also called intra-group perception tokens, which represent the model’s fine-grained perception towards the same video content. Our goal is to model the importance of these tokens, allowing the policy model to prioritize the learning of tokens in higher rewards responses while suppressing those in lower rewards responses. Inspired by recent works [23, 24], which demonstrate that key reasoning tokens can be identified based on token-level distributional differences, we argue that these intra-group perception tokens could be treated as crucial fine-grained tokens, and they should be given different learning intensities based on information differences among them.

In particular, we first formally define intra-group perception tokens as follows:

$$\Omega = \{\Omega^{(1)}, \Omega^{(2)}, \dots, \Omega^{(K)}\}, \quad (9)$$

$$\Omega^{(k)} = \left\{ \text{TopK}_{o_{i,j}} \left( \text{Attn}(o_{i,j}, f_k), K_3 \right) \right\}_{i=1}^G, \quad (10)$$

where  $\Omega$  represents  $K$  groups of tokens, each group focusing on a frame  $f_k$  in  $\psi'$  and  $K = |\psi'|$ ,  $\Omega^{(k)}$  denotes the set of  $G \times K_3$  tokens selected from each response  $o_i$  that have the highest attention to a specific frame in  $\psi'$ . A more illustrative diagram is shown in Fig. 4. To measure the token discrepancy within  $\Omega^{(k)}$ , the Kullback-Leibler (KL) divergence is used to compute the probability distribution differences, which can be formalized as:

$$D^{(k)} = \sum_{i=1}^G D_{\text{KL}} \left( p(\Omega_{i,j}^{(k)}) \parallel \mathbb{E}[\Omega_j^{(k)}] \right), \quad (11)$$

where  $\mathbb{E}[\Omega_j^{(k)}]$  is computed by averaging the probability distribution of each response within  $\Omega^{(k)}$ , and the  $D^{(k)}$  represents the importance weight of each token within  $\Omega^{(k)}$ . We normalize  $D^k$  using min-max normalization to ensure the numerical stability. The final token importance weight is averaged by  $K$  groups:

$$\mathcal{W} = 1 + \alpha \cdot \frac{1}{K} \sum_{k=1}^K D^{(k)}, \quad (12)$$

where  $\alpha$  is a hyperparameter that controls the scaling of token weights.

To this end, the resulting weights  $\mathcal{W}$  enable fine-grained perception-aware optimization by modulating the learning of token-level perception signals. Following DAPO, we remove the KL divergence constraint to enhance the model’s exploratory capabilities, and normalize the number of outputs  $o_i$  to balance their contributions to the overall loss. Therefore, the policy model is optimized with the following objective (we omit the clip term for

---

**Algorithm 1** Attention-guided Perception Policy Optimization (APPO)
 

---

**Require:**

- $\pi_\theta$ : Online policy model (initialized from pretrained weights)
  - $\mathcal{D}$ : Multimodal training dataset  $\{\mathcal{V}, q, a\}$
  - $\tau$ : reward threshold (e.g., 0.5)
  - $K_1, K_2, K_3$ : hyper-parameters for TopK selection (e.g., 15, 5, 64)
  - $\alpha$ : hyper-parameter to control the scaling of token weights
- 1: **procedure** TRAINING( $\pi_\theta, \mathcal{D}, T$ )
  - 2:   **for**  $t \leftarrow 1$  to  $T$  **do**
  - 3:     **for** each multimodal input  $x$  in  $\mathcal{D}$  **do**
  - 4:       **Step 1: Generation & Rewards Computation**
  - 5:        Generate  $G$  responses:  $\{o_i\}_{i=1}^G \sim \pi_\theta(\cdot|x)$
  - 6:        Compute format and accuracy rewards:  $\{r_i\}_{i=1}^G$
  - 7:        Divide  $G$  responses into two sets  $S_1$  and  $S_2$  based on format rewards in Eq. 3
  - 8:        **Step 2: Frame Selection based on Attention**
  - 9:        Compute attention weights to video frame in Eq. 4
  - 10:       Compute video frame indices that are most focused by  $S_1$  and  $S_2$  in Eq. 6 7 8
  - 11:       Employ one select strategy to get  $\psi'$
  - 12:       **Step 3: Perception Tokens Re-weighting**
  - 13:       Measure token discrepancy  $D^{(k)}$  using  $KL$  divergence in Eq. 14
  - 14:       Normalize the divergence measurements using min-max normalization:  $\mathcal{D}^{(k)} = \frac{D^{(k)} - D_{min}^{(k)}}{D_{max}^{(k)} - D_{min}^{(k)}}$
  - 15:       Average final token weights  $\mathcal{W}$  in Eq. 12
  - 16:       Compute APPO loss in Eq. 13 to optimize  $\pi_\theta$
  - 17:     **end for**
  - 18:   **end for**
  - 19:   **return** optimized policy  $\pi_\theta$
  - 20: **end procedure**
- 

simplicity):

$$\mathcal{L}_{\text{APPO}} = \mathbb{E}_{o \sim \pi_\theta^{\text{old}}} \left[ \frac{1}{\sum_{i=1}^G |o_i|} \sum_{i=1}^G \sum_{t=1}^{|o_i|} r_{i,t}(\theta) \cdot \mathcal{W} \cdot A_i \right]. \quad (13)$$

Above process is shown in Algorithm 1. More details can be found in *supplementary materials*.

## 4 Experiments

### 4.1 Experimental Setup

**Evaluation.** To validate the effectiveness of our proposed APPO, we conduct evaluations on diverse video benchmarks, including: (1) video reasoning tasks (e.g., SEED-Bench-R1 [9], VSI-Bench [27], Perception Test [10]);

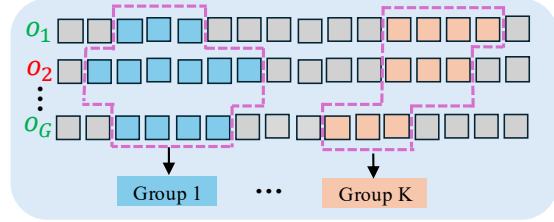


**Figure 4** The illustration of intra-group perception tokens. The tokens within the same group primarily focus on the same crucial video frame.

(2) fine-grained spatial-temporal video reasoning tasks (NExT-GQA [28]) and (3) general video understanding tasks (e.g., MVBench [29], NExT-QA [30]).

**Implementation details.** We perform direct RL training from Qwen2.5-VL-3B and 7B models, comparing the standard GRPO and DAPO baseline with our proposed APPO. We use the accuracy and format rewards to train the model on 6K SEED-Bench-R1 and 6K Perception Test multi-choice training subset for 1 epoch, respectively. The IoU reward is added to train models on 3K NExT-GQA validation set for 2 epochs. The weights of three rewards are 0.9, 0.1, and 0.9. For zero-shot evaluation on VSI-Bench, MVBench and NExT-QA, we select a subset of 34K training data from Video-R1-260K RL dataset and train the model for 1 epoch. The rollout numbers for per input sample in set to 8. APPO uses the same clip-higher strategy as DAPO and dynamic sampling strategy was not used. Training batch size is 16 and learning rate is fixed as  $1e-6$ . Each frame is processed at a resolution of  $224 \times 224$  while maintaining a maximum of 30 frames for 3B model and 16 frames for 7B model during training. We only use accuracy reward scores to group all responses, and the reward threshold  $\tau$  in Eq. 3 is set to 0.5. More training details are provided in the *supplementary materials*.

### 4.2 Main Results

To verify the effectiveness of APPO, we compared with SFT, GRPO and DAPO based on the same dataset and base model (Qwen2.5-VL-3/7B) to ensure a fair evaluation. The main results are shown in Table. 1.

**RL generally enhances performance compared to SFT.** It can be found that RL methods such as GRPO, DAPO, and APPO have effectively improved model performance compared to traditional SFT, both in video understanding and reasoning benchmarks, indicating the significant advancements in recent RL explorations.

**Overall performance improvement compared to GRPO and DAPO on diverse video benchmarks.** APPO consistently outperforms GRPO and DAPO on video reasoning and general understanding benchmarks. Specif-

**Table 1** The comparison results across SFT, GRPO, DAPO and our APPO based on diverse video benchmarks and Qwen2.5-VL-3/7B models. All experiments are conducted on the same dataset and experimental settings to ensure a fair comparison. For evaluation, each frame is processed at a resolution of  $224 \times 224$ . The video is sampled at  $1fps$  while maintaining the maximum of 60 frames.

Method	SEED-Bench-R1				NExTGQA		Perception Test	VSI-Bench	MVBench	NExT-QA
	L1 (In-Dist.)	L2 (OOD)	L3 (OOD)	Avg.	mIoU	Acc@QA				
<b>Qwen2.5-VL-3B</b>										
Base Model	28.2	29.4	27.0	28.0	10.1	40.3	42.9	29.2	50.8	59.4
+ SFT	32.6	33.7	28.6	31.6	10.5	63.7	58.2	32.9	57.1	72.4
+ GRPO	35.3	35.7	31.0	34.0	10.3	70.7	62.1	34.8	61.5	74.2
+ DAPO	<u>36.6</u>	<u>37.5</u>	<u>31.8</u>	<u>35.3</u>	<u>10.6</u>	<u>70.9</u>	<u>62.5</u>	<u>36.7</u>	<b>62.8</b>	<u>76.1</u>
<b>+ APPO (Ours)</b>	<b>37.5</b>	<b>39.1</b>	<b>35.0</b>	<b>37.2</b>	<b>11.1</b>	<b>71.2</b>	<b>63.1</b>	<b>38.2</b>	<u>62.4</u>	<b>76.4</b>
<b>Qwen2.5-VL-7B</b>										
Base Model	29.1	32.7	29.6	30.5	13.5	49.9	55.2	27.8	56.4	67.6
+ SFT	40.2	42.8	43.9	42.3	28.4	72.1	60.2	31.8	58.2	72.4
+ GRPO	49.0	49.7	48.2	48.9	32.0	<u>75.1</u>	66.0	35.9	63.2	78.4
+ DAPO	<u>50.0</u>	<u>51.3</u>	<u>48.7</u>	<u>50.0</u>	<u>32.4</u>	75.0	<u>66.4</u>	<u>36.6</u>	<u>64.2</u>	<b>79.9</b>
<b>+ APPO (Ours)</b>	<b>50.5</b>	<b>51.6</b>	<b>49.3</b>	<b>50.5</b>	<b>32.9</b>	<b>75.8</b>	<b>66.9</b>	<b>36.9</b>	<b>64.6</b>	<u>79.6</u>

**Table 2** The comparison results with video reasoning models on diverse video benchmarks. Our APPO is trained on a subset of  $34K$  from Video-R1-260K dataset. All methods employ the same base model Qwen2.5-VL-7B for zero-shot evaluation on these benchmarks. For evaluation, each frame is processed at a resolution of  $224 \times 224$ . The video is sampled at  $1fps$  with the maximum of 30 frames.

Method	Size	Training Data	SEED-Bench-R1				NExTGQA		Perception Test	VSI-Bench	MVBench	NExT-QA
			L1 (In-Dist.)	L2 (OOD)	L3 (OOD)	Avg.	mIoU	Acc@QA				
<b>Video Reasoning Models</b>												
TW-GRPO [8]	7B	1K	30.2	29.0	25.6	28.3	17.7	53.2	54.9	25.1	52.9	70.2
VideoChat-R1 [25]	7B	18K	<u>33.3</u>	<u>34.4</u>	27.8	<u>31.8</u>	<b>22.0</b>	63.2	57.7	19.9	55.8	74.5
GRPO-CARE [7]	7B	260K	29.9	28.3	26.0	28.1	<u>18.0</u>	51.5	57.1	24.0	54.6	66.4
Video-R1 [5]	7B	260K	30.9	32.3	28.8	30.7	14.9	64.7	57.0	<b>35.8</b>	<u>63.9</u>	76.5
VideoRFT [26]	7B	310K	32.4	32.5	27.7	30.9	14.4	<u>72.0</u>	<u>60.4</u>	30.3	59.0	<u>78.3</u>
<b>APPO (Ours)</b>	7B	34K	<b>35.4</b>	<b>40.0</b>	<b>34.7</b>	<b>36.1</b>	16.9	<b>76.3</b>	<b>64.7</b>	<u>32.7</u>	<b>64.6</b>	<b>79.2</b>

ically, for video reasoning tasks, such as SEED-Bench-R1 and VSI-Bench, APPO demonstrated a significant performance improvement (1.5%  $\sim$  3.2% on 3B model and 0.3%  $\sim$  1.6% on 7B model). On general video understanding dataset, including MVBench and NExT-QA, APPO achieved comparable performance. For fine-grained spatiotemporal perception tasks, *e.g.* NExT-GQA, APPO shows overall performance improvements on mIoU and accuracy metrics.

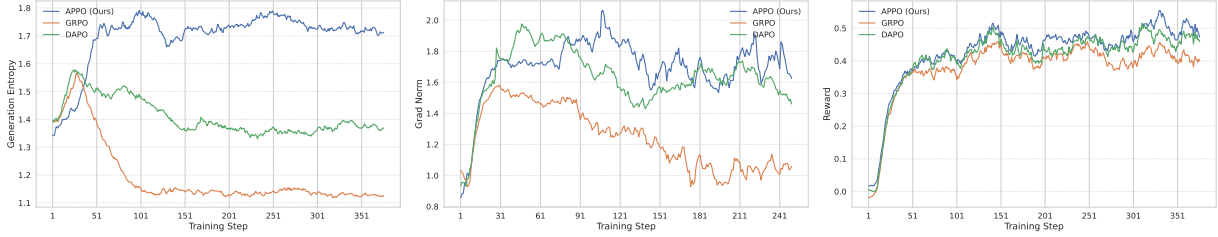
**APPO demonstrates greater advantages in enhancing fine-grained perception capabilities.** It is worth noting that the performance improvement on the 7B model is not as remarkable as on the 3B model on SEED-Bench-R1 benchmark (0.5% *vs.* 1.9% compared with DAPO, 1.6% *vs.* 3.2% compared with GRPO). We attribute this to the weaker perception capabilities of the 3B model, where the advantage of APPO in enhancing fine-grained perception is more prominently displayed. This phenomenon is also reflected in the NExT-GQA dataset, where the mIoU metric primarily measures the model’s fine-grained spatiotemporal perception capabilities. It can be observed that the GRPO and DAPO algorithms have limited performance improvements in grounding the correct frames (0.2% and 0.4% improvements on 3B model). In comparison, APPO could achieve improvements of 1.0% on 3B

model, and the consistent conclusion is also drawn for the 7B model.

**Stronger generalization capabilities.** For OOD test data (Level-2 and Level-3) on SEED-Bench-R1 benchmark, where the testing data comes from Ego4D [31], including cross-environment tasks, APPO achieved a more remarkable improvement over DAPO (1.6% and 3.2% on 3B model), which is significantly greater than performance improvement on Level-1 in-distribution test data (0.9% on 3B model), demonstrating stronger generalization capabilities.

### 4.3 Comparison with other video reasoning models

To verify the advantages of our APPO algorithm compared to existing works, we selected a subset of  $34K$  training data from the Video-R1-260K RL dataset and trained the Qwen2.5-VL-7B model using APPO algorithm. Detailed composition of training data is provided in the *supplementary materials*. Table. 2 shows the comparison results of APPO with existing video reasoning models, including TW-GRPO [8], GRPO-CARE [7], Video-R1 [5], VideoRFT [26] and VideoChat-R1 [25]. We also present the training data scales for these models. All methods em-



(a) The comparison of generation entropy. (b) The comparison of grad norm. (c) The comparison of reward score.  
**Figure 5** The comparison of generation entropy, grad norm and reward scores during training process with GRPO and DAPO.

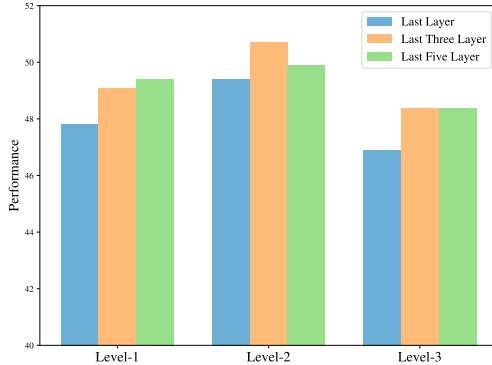


**Figure 6** The ablation results for different attention layers.

ploy the same base model Qwen2.5-VL-7B for zero-shot evaluation on these benchmarks.

It can be observed that while APPO is trained on only a small dataset of 34K, it demonstrates overall performance improvements compared to other methods trained on larger-scale datasets. In particular, the APPO achieves the superior results on the SEED-Bench-R1, Perception Test, VSI-Bench, MVBench, and NEX-T-QA benchmarks, yielding a performance improvement of 0.7% ~ 5.2%, which demonstrates the remarkable advantages of APPO in enhancing fine-grained perception during reasoning. For NEX-T-GQA benchmark, the training data for Video-Chat-R1 includes temporal grounding tasks, which significantly enhances its temporal grounding ability. Compared to other models, APPO achieves comparable performance, particularly excelling in multi-choice accuracy (76.3%). The overall performance improvement achieved by APPO demonstrates the effectiveness of enhancing fine-grained perception.

#### 4.4 Comparison and analysis of training process

To further understand the training process of APPO, we compared and analyzed the dynamic changes of generation entropy, gradient norm, and reward scores with GRPO and DAPO during training process. As shown in Fig. 5, it can be observed that during the training process, APPO exhibits higher generation entropy and grad norm, indicat-

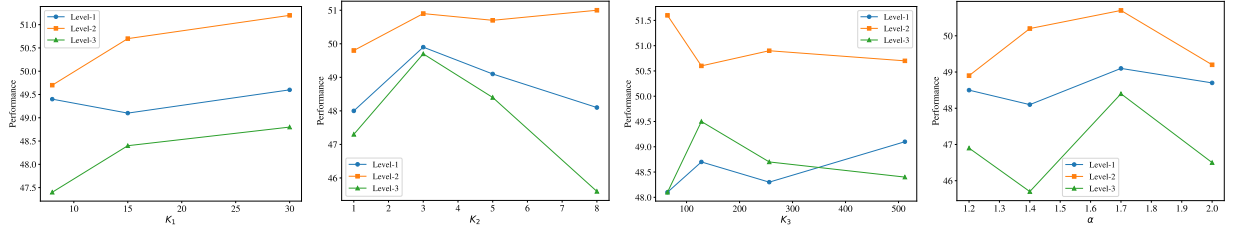
ing the model has a larger exploration space. We attribute this phenomenon to the gains brought about by optimizing those intra-group perception tokens. The reward score curve in Fig. 5c also indicates APPO has higher rewards, resulting in superior performance.

#### 4.5 Ablation study for APPO

To analyze impact of hyperparameters in APPO algorithm, we conducted comprehensive ablation experiments based on SEED-Bench-R1 dataset and Qwen2.5-VL-7B model as follows, mainly including: (1)  $K_1$  in Eq. 6; (2)  $K_2$  in Eq. 7; (3)  $K_3$  in Eq. 10; (4)  $\alpha$  in Eq. 12 and (5) attention layers to compute attention weights. More ablation experiments, such as three select strategies, are provided in *supplementary materials*.

**Ablation results for  $K_1, K_2$  and  $K_3$ .** As shown in Fig. 7a, a larger  $K_1$  generally leads to overall performance improvements because it can more accurately represent the attention weights of response  $o_i$  on video frames, enhancing the reliability of selected frames. In Fig. 7b, there is an optimal value for  $K_2$ , which is  $K_2 = 3$ . The possible reason is that smaller  $K_2$  might lead to missing some important frames, while larger  $K_2$  could increase the number of selected frames, introducing frame noise and misleading the optimization direction. For  $K_3$  in Fig. 7c, larger  $K_3$  means that more perception tokens are selected in each response. However, since the content of each frame is limited, too many tokens are unnecessary and could interfere with the model’s optimization of truly useful perception tokens.

**Ablation results for  $\alpha$ .** The  $\alpha$  in Eq. 12 controls the regulation strength of perception tokens. As shown in Fig. 7d, as  $\alpha$  increases from 1.2 to 2.0, the performance across three levels first increases and then decreases, reaching a maximum when  $\alpha = 1.7$ . Moreover, the variation in  $\alpha$  has a greater impact on OOD test data (maximum performance difference 1.8% on L2 and 2.7% on L3) compared to in-distribution data (maximum performance difference 1%), indicating a close relationship between optimization strength of tokens and generalization capabilities.



(a) Ablation results for  $K_1$ . (b) Ablation results for  $K_2$ . (c) Ablation results for  $K_3$ . (d) Ablation results for  $\alpha$ .  
**Figure 7** The ablation results for different hyperparameters in APPO based on SEED-Bench-R1 benchmark and Qwen2.5-VL-7B model.

**Ablation results for attention layers.** In Eq. 4, we need to calculate the average attention scores across several layers to obtain the attention weights. To explore the impact of attention layers on performance, we compared three strategies: the last layer, the last three layers and the last five layers. As shown in Fig. 6, using only the last layer results in the worse performance, possibly due to the lack of sufficiently accurate attention information. As the number of attention layers increases from 3 to 5, there is a gradual improvement in performance. However, considering training efficiency, an excessive number of attention layers can consume more GPU memory. Therefore, using the last three layers might be the optimal choice.

## 5 Conclusion

In this work, we innovatively decouple the model’s perception and reasoning capabilities. Through extensive experimental observations, we found that enhancing perception abilities could bring more significant improvements compared to enhancing reasoning. Building upon this observation, to fully enhance the model’s fine-grained perception abilities during reasoning process, we propose the APPO algorithm, which utilizes token-level fine-grained rewards to optimize the model. Experimental results on diverse video benchmarks and models of different scales consistently show that APPO is more suitable for video reasoning tasks compared to mainstream algorithms like GRPO and DAPO. Our work provides a promising approach to effectively enhance model’s perception abilities through reasoning in a low-cost manner, serving diverse scenarios.

## References

- [1] A. Jaech, A. Kalai, A. Lerer, A. Richardson, A. El-Kishky, A. Low, A. Helyar, A. Madry, A. Beutel, A. Carney *et al.*, “Openai o1 system card,” *arXiv preprint arXiv:2412.16720*, 2024.
- [2] D. Guo, D. Yang, H. Zhang, J. Song, R. Zhang, R. Xu, Q. Zhu, S. Ma, P. Wang, X. Bi *et al.*, “Deepseek-r1: Incentivizing reasoning capability in llms via reinforcement learning,” *arXiv preprint arXiv:2501.12948*, 2025.
- [3] Q. Yu, Z. Zhang, R. Zhu, Y. Yuan, X. Zuo, Y. Yue, W. Dai, T. Fan, G. Liu, L. Liu *et al.*, “Dapo: An open-source llm reinforcement learning system at scale,” *arXiv preprint arXiv:2503.14476*, 2025.
- [4] C. Zheng, S. Liu, M. Li, X.-H. Chen, B. Yu, C. Gao, K. Dang, Y. Liu, R. Men, A. Yang *et al.*, “Group sequence policy optimization,” *arXiv preprint arXiv:2507.18071*, 2025.
- [5] K. Feng, K. Gong, B. Li, Z. Guo, Y. Wang, T. Peng, J. Wu, X. Zhang, B. Wang, and X. Yue, “Video-r1: Reinforcing video reasoning in mllms,” *arXiv preprint arXiv:2503.21776*, 2025.
- [6] J. Park, J. Na, J. Kim, and H. J. Kim, “Deepvideo-r1: Video reinforcement fine-tuning via difficulty-aware regressive grpo,” *arXiv preprint arXiv:2506.07464*, 2025.
- [7] G. GRPO-CARE, “Grpo-care: Consistency-aware reinforcement learning for multimodal reasoning.”
- [8] J. Dang, J. Wu, T. Wang, X. Lin, N. Zhu, H. Chen, W.-S. Zheng, M. Wang, and T.-S. Chua, “Reinforcing video reasoning with focused thinking,” *arXiv preprint arXiv:2505.24718*, 2025.
- [9] Y. Chen, Y. Ge, R. Wang, Y. Ge, L. Qiu, Y. Shan, and X. Liu, “Exploring the effect of reinforcement learning on video understanding: Insights from seed-bench-r1,” *arXiv preprint arXiv:2503.24376*, 2025.
- [10] V. Patraucean, L. Smaira, A. Gupta, A. Recasens, L. Markeeva, D. Banarse, S. Koppula, M. Malinowski, Y. Yang, C. Doersch *et al.*, “Perception test: A diagnostic benchmark for multimodal video models,” *Advances in Neural Information Processing Systems*, vol. 36, pp. 42 748–42 761, 2023.
- [11] S. Bai, K. Chen, X. Liu, J. Wang, W. Ge, S. Song, K. Dang, P. Wang, S. Wang, J. Tang *et al.*, “Qwen2. 5-vl technical report,” *arXiv preprint arXiv:2502.13923*, 2025.
- [12] G. Comanici, E. Bieber, M. Schaeckermann, I. Pasupat, N. Sachdeva, I. Dhillon, M. Blistein, O. Ram, D. Zhang, E. Rosen *et al.*, “Gemini 2.5: Pushing the frontier with advanced reasoning, multimodality, long context, and next generation agentic capabilities,” *arXiv preprint arXiv:2507.06261*, 2025.
- [13] A. Yang, A. Li, B. Yang, B. Zhang, B. Hui, B. Zheng, B. Yu, C. Gao, C. Huang, C. Lv *et al.*, “Qwen3 technical report,” *arXiv preprint arXiv:2505.09388*, 2025.
- [14] S. Li, K. Deng, L. Wang, H. Yang, C. Peng, P. Yan, F. Shen, H. T. Shen, and X. Xu, “Truth in the few: High-value data selection for efficient multi-modal reasoning,” *arXiv preprint arXiv:2506.04755*, 2025.
- [15] T. Liang, X. Liu, P. He, H. Mi, Z. Tu, and D. Y. Modomodo, “Learning mixture-of-datasets with reinforcement learning for multimodal reasoning,” *arXiv preprint arXiv:2505.24871*, vol. 1, no. 2, p. 10, 2025.
- [16] Y. Wang, Z. Wang, B. Xu, Y. Du, K. Lin, Z. Xiao, Z. Yue, J. Ju, L. Zhang, D. Yang *et al.*, “Time-r1: Post-training large vision language model for temporal video grounding,” *arXiv preprint arXiv:2503.13377*, 2025.
- [17] K. Ouyang, Y. Liu, H. Wu, Y. Liu, H. Zhou, J. Zhou, F. Meng, and X. Sun, “Spacer: Reinforcing mllms in video spatial reasoning,” *arXiv preprint arXiv:2504.01805*, 2025.
- [18] M. Cao, H. Zhao, C. Zhang, X. Chang, I. Reid, and X. Liang, “Ground-r1: Incentivizing grounded visual reasoning via reinforcement learning,” *arXiv preprint arXiv:2505.20272*, 2025.
- [19] Z. Zheng, M. Yang, J. Hong, C. Zhao, G. Xu, L. Yang, C. Shen, and X. Yu, “Deepeyes: Incentivizing “thinking with images” via reinforcement learning,” *arXiv preprint arXiv:2505.14362*, 2025.
- [20] H. Zhang, X. Gu, J. Li, C. Ma, S. Bai, C. Zhang, B. Zhang, Z. Zhou, D. He, and Y. Tang, “Thinking with videos: Multimodal tool-augmented reinforcement learning for long video reasoning,” *arXiv preprint arXiv:2508.04416*, 2025.
- [21] J. Xia, Y. Zang, P. Gao, Y. Li, and K. Zhou, “Visionary-r1: Mitigating shortcuts in visual reasoning with reinforcement learning,” *arXiv preprint arXiv:2505.14677*, 2025.
- [22] T. Xiao, X. Xu, Z. Huang, H. Gao, Q. Liu, Q. Liu, and E. Chen, “Advancing multimodal reasoning capabilities of multimodal large language models via visual perception reward,” *arXiv preprint arXiv:2506.07218*, 2025.
- [23] E. Bigelow, A. Holtzman, H. Tanaka, and T. Ullman, “Forking paths in neural text generation,” *arXiv preprint arXiv:2412.07961*, 2024.
- [24] Z. Lin, T. Liang, J. Xu, Q. Lin, X. Wang, R. Luo, C. Shi, S. Li, Y. Yang, and Z. Tu, “Critical tokens matter: Token-level contrastive estimation enhances llm’s reasoning capability,” *arXiv preprint arXiv:2411.19943*, 2024.
- [25] X. Li, Z. Yan, D. Meng, L. Dong, X. Zeng, Y. He, Y. Wang, Y. Qiao, Y. Wang, and L. Wang, “Videochat-r1: Enhancing spatio-temporal perception via reinforcement fine-tuning,” *arXiv preprint arXiv:2504.06958*, 2025.
- [26] Q. Wang, Y. Yu, Y. Yuan, R. Mao, and T. Zhou, “Videorf1: Incentivizing video reasoning capability in mllms via reinforced fine-tuning,” *arXiv preprint arXiv:2505.12434*, 2025.

- [27] J. Yang, S. Yang, A. W. Gupta, R. Han, L. Fei-Fei, and S. Xie, “Thinking in space: How multimodal large language models see, remember, and recall spaces,” in *Proceedings of the Computer Vision and Pattern Recognition Conference*, 2025, pp. 10 632–10 643.
- [28] J. Xiao, A. Yao, Y. Li, and T.-S. Chua, “Can i trust your answer? visually grounded video question answering,” in *Proceedings of the IEEE/CVF Conference on Computer Vision and Pattern Recognition*, 2024, pp. 13 204–13 214.
- [29] K. Li, Y. Wang, Y. He, Y. Li, Y. Wang, Y. Liu, Z. Wang, J. Xu, G. Chen, P. Luo *et al.*, “Mvbench: A comprehensive multi-modal video understanding benchmark,” in *Proceedings of the IEEE/CVF Conference on Computer Vision and Pattern Recognition*, 2024, pp. 22 195–22 206.
- [30] J. Xiao, X. Shang, A. Yao, and T.-S. Chua, “Next-qa: Next phase of question-answering to explaining temporal actions,” in *Proceedings of the IEEE/CVF conference on computer vision and pattern recognition*, 2021, pp. 9777–9786.
- [31] K. Grauman, A. Westbury, E. Byrne, Z. Chavis, A. Furnari, R. Girdhar, J. Hamburger, H. Jiang, M. Liu, X. Liu *et al.*, “Ego4d: Around the world in 3,000 hours of egocentric video,” in *Proceedings of the IEEE/CVF conference on computer vision and pattern recognition*, 2022, pp. 18 995–19 012.
- [32] J. Zhang, M. Khayatkhoei, P. Chhikara, and F. Ilievski, “Mllms know where to look: Training-free perception of small visual details with multimodal llms,” *arXiv preprint arXiv:2502.17422*, 2025.
- [33] W. Kwon, Z. Li, S. Zhuang, Y. Sheng, L. Zheng, C. H. Yu, J. Gonzalez, H. Zhang, and I. Stoica, “Efficient memory management for large language model serving with pagedattention,” in *Proceedings of the 29th symposium on operating systems principles*, 2023, pp. 611–626.

# Appendix

## A Details of APPO

Our APPO algorithm primarily consists of two core steps: Attention-guided Frame Selection and Intra-group Perception Tokens Re-weighting, as mentioned in Section 3.2 of main submission. Therefore, in this section, we mainly discuss rationality and correctness of these two steps in detail.

### A.1 Attention-guided Frame Selection

To understand the limitations of MLLMs’ visual perception, recent works [32] have studied the attention patterns of MLLMs when answering visual questions. Inspired by these works, we also explored the attention patterns in video scenarios. The Fig. H and Fig. J present the attention patterns of response tokens to the video frames, respectively. It can be found that: (1) For the same video, the model exhibits different patterns of attention weights on video frames as the question changes; (2) The model’s incorrect answers are due to either missing crucial frames or assigning too low attention weights to these frames. In particular, as shown in Fig. H, the question is “What is the mouse writing on the blackboard?”, and the answer mainly appears in the last part of the video. The model correctly focused on the last few frames, especially when it provided correct information such as “very nice”. Similarly, in Fig. J, the question is “What is the kitten doing when the blue cat turns its head for the second time?”, and the answer mainly appears in the middle part of the video (16s ~ 21s). Clearly, the model did not pay sufficient attention to these video frames, resulting in an incorrect answer.

These empirical observations inspire us that the reasoning paths with higher rewards are more likely to focus on crucial frames. Therefore, as mentioned in Section 3.2 of main submission, we can divide all reasoning paths into two sets based on the reward scores, and then utilize the attention differences between these two sets to obtain frame-level guiding signals.

### A.2 Intra-group Perception Tokens Re-weighting

The main goal of this step is to determine different learning intensities for intra-group perception tokens. Recent works [23, 24] demonstrate that the key reasoning tokens can be identified based on token-level distributional differences. Building upon this conclusion, Jisheng *et al.* [8] calculated the weights of tokens at each position for the entire sequence. Similarly, we argue that the intra-group perception tokens for each crucial frame could be treated

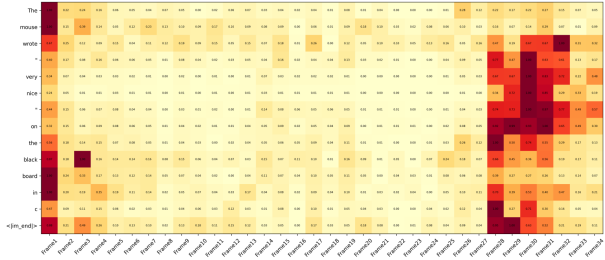


**Figure H** The attention weights of response tokens to video frames. Question: “What did the mouse write on the blackboard?”. The answer mainly appears in the last part of the video. The x-axis represents the video frame index (total 34 frames). The y-axis shows the response tokens. The darker the color, the higher the attention score.

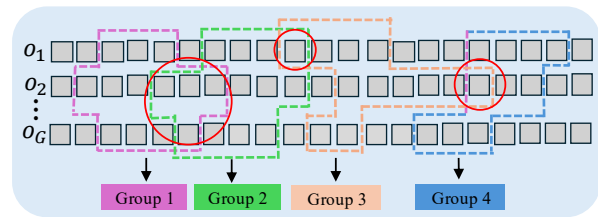


**Figure I** The illustration of four intra-group perception tokens. The same token may attend to multiple crucial frames, as shown in the red solid circles in the figure.

as crucial fine-grained perception tokens, and they should be given different learning intensities based on information differences among them.

In particular, for each crucial frame  $\mathcal{I}$  in  $\psi'$ , each path contains certain perception tokens that focus primarily on this frame. The importance weights of this group of tokens at each position can be computed as follows:

$$D^{(k)} = \sum_{i=1}^G D_{\text{KL}} \left( p(\Omega_{i,j}^{(k)}) \parallel \mathbb{E}[\Omega_j^{(k)}] \right), \quad (14)$$

where  $\mathbb{E}[\Omega_j^{(k)}]$  is computed by averaging the probability distribution of each response within  $\Omega^{(k)}$ , and the  $D^{(k)}$  represents the importance weight of each token within  $\Omega^{(k)}$ . Since the same token may attend to several crucial frames in  $\psi'$ , these tokens may correspond to multiple optimization intensities, as shown in the red solid circles in Fig. I. Therefore, we additionally record the numbers of each token is optimized and the cumulative sum of the optimization intensities, then leverage the average intensity as the final token weights.

## B Detailed Experimental Setup

For RL training, we limit the maximum number of response tokens to 512 for training efficiency. Each training

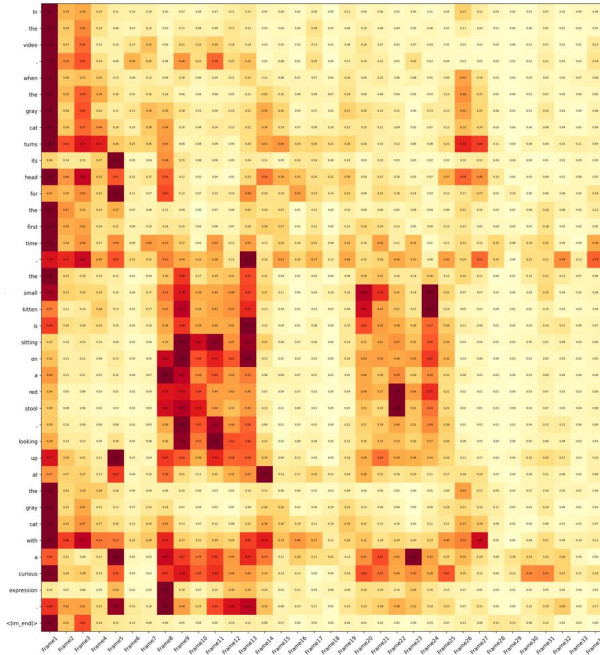


**Figure J** The attention weights of response tokens to video frames. Question: “When the blue cat turned his head to look the second time, what was the small kitten doing?”. The answer mainly appears in the middle part of the video (15s ~ 20s). The x-axis represents the video frame index (total 34 frames). The y-axis shows the response tokens. The darker the color, the higher the attention score.

step processes 16 input samples, with 8 rollouts per sample. Rollout sampling uses a temperature of 1.0 and top-p of 1.0. Specifically, for GRPO, we use a KL divergence coefficient of 0.01. For DAPO, the clip higher is set to 0.28. For our APPO, to obtain attention weights, we set the model’s attention implementation to “eager” during sampling and average the weights across all attention heads. We use the official Hugging Face TRL library for training.

For evaluation, we use the vLLM [33] inference engine to accelerate, with a sampling temperature of 0.1, top-p of 0.001, top-k of 1, and a repetition penalty of 1.05. For accuracy calculation, we use regular expressions to match the predicted results with the ground truth. For mIoU calculation, we strictly compute the intersection and union between the predicted results and the labels.

Detailed hyperparameters during training and evaluation are shown in Tab. C.

## C Training Data Composition

To validate the effectiveness of our APPO compared to GRPO and DAPO, we collected subsets from existing dataset for RL training, including: 6K SEED-Bench-R1

**Table C** The hyperparameters used during training and evaluation.

Hyper-parameters	Value
<b>Training</b>	
Batch size	16
Gradient Accumulation Steps	1
Warmup	False
Rollout Numbers	8
Rollout Temperature	1.0
Rollout Top-P	1.0
Freeze Vision Encoder	True
KL divergence coefficient	$1 \times 10^{-2}$
Learning rate	$1 \times 10^{-6}$
GPUs	16
Optimizer	AdamW
Training Framework	TRL
<b>Evaluation</b>	
Inference Engine	vLLM
Temperature	0.1
Top-P	0.001
Top-K	1
Repetition Penalty	1.05

**Table D** The detailed composition of 34K training subset selected from Video-R1-260K RL training data.

Data Resource	Sample Num.
LLaVA-Video	~ 5K
STAR	~ 11K
Perception Test	~ 6K
NExT-QA	~ 5K
CLEVRER	~ 6K

training subset, 6K Perception Test multiple-choice subset, 3K NExT-GQA validation subset. To compare APPO with other video reasoning models, we selected 34K subset from Video-R1-260K RL training data, as summarized in Tab. D.

## D Additional Experiment Results

To investigate the impact of the three selection strategies on the APPO algorithm, we conducted ablation experiments on SEED-Bench-R1 benchmark, as shown in Tab. E. It can be observed that the Soft selection strategy performs the best, as it can fully promote fine-grained perception learning in both the high reward path set and the low reward path set.

For example, since APPO relies on the model’s attention scores, this means that when sampling multiple reasoning paths, the model’s attention implementation must be “eager.” Additionally, existing inference acceleration

**Table E** Ablation results for different select strategies on SEED-Bench-R1 Benchmark.

Strategy	L1 (In-Dist.)	L2 (OOD)	L3 (OOD)
Hard	49.1	50.7	48.4
Soft	<b>50.5</b>	<b>51.3</b>	<b>49.3</b>
All	50.2	50.9	47.3

**Table F** The training efficiency comparison between DAPO and our APPO. Training efficiency refers to the training samples processed per second.

Model Scale	Training Efficiency		Percentage
	DAPO	APPO (Ours)	
3B (30 frames)	0.325	0.264	81%
7B (16 frames)	0.462	0.429	93%

frameworks, such as vLLM, have difficulty supporting the retrieval of attention scores, which limits the efficiency of the APPO algorithm.

## E Prompt Template

The prompt templates used for RL training on different tasks are as follows.

Prompt Template for Temporal Video Grounding Task
<p>The video is {duration} seconds long, with {frame_nums} frames evenly sampled from it.</p> <p>Based on the video content, think about the question deeply, select the correct option, and provide ONE or MORE time periods in the video where the clues corresponding to the correct option occur.</p> <p>Question: {Question}</p> <p>Output the thinking process in &lt;think&gt; &lt;/think&gt; tags, final answer in &lt;answer&gt; &lt;/answer&gt; tags and time clues in &lt;time&gt; &lt;/time&gt; tags, i.e., &lt;think&gt; reasoning process here &lt;/think&gt; &lt;answer&gt; answer here &lt;/answer&gt; &lt;time&gt; 8.4 to 12.5, 25 to 30.2 &lt;/time&gt;</p>

**Figure K** The prompt template for temporal video grounding task.

Prompt Template for RL Training
<p>{Question} Output the thinking process in &lt;think&gt; &lt;/think&gt; and final answer in &lt;answer&gt; &lt;/answer&gt; tags, i.e., &lt;think&gt; reasoning process here &lt;/think&gt;&lt;answer&gt; answer here &lt;/answer&gt;."</p>

**Figure L** The prompt template for RL training.

## F Visualization Results

As shown in Fig. M, we present visualization example from SEED-Bench-R1 Level-3 testset. It can be found that while GRPO and DAPO algorithms correctly answered question, it is noteworthy that our APPO algorithm successfully paid attention to the critical information of *hand-washing*, which made the subsequent logical reasoning more coherent.

## G Limitations

While APPO achieves superior results than GRPO and DAPO in complex video reasoning scenarios, it also has some limitations. For example, since APPO relies on the model’s attention scores, this means that when sampling multiple reasoning paths, the model’s attention implementation must be “eager”. Additionally, existing inference acceleration frameworks, such as vLLM, have difficulty supporting the output of attention scores. However, based on our experimental statistics, the training efficiency of APPO is 81% ~ 93% that of DAPO under the same training data and model scale, as shown in Tab. F. We will propose effective solutions to mitigate this limitation in the future works.

**Question:** Considering the progress shown in the video and my current observation shown in the image, what action should I take next in order to prepare bread? A. rotate frying pan B. pick plates C. adjust plates D. turn off sink tap



**GRPO:** <think> The video shows that the person is preparing food on the stove. The next logical step would be to ensure the cooking area is clean and organized. Turning off the sink tap is a necessary action to prevent any water from splashing onto the stove or other cooking surfaces. This ensures safety and prevents any potential accidents. </think>\n<answer> D </answer>

**DAPO:** <think> The video shows that the person is preparing food on the stove and has just finished cooking something in a frying pan. The next logical step in preparing bread would be to clean up the kitchen area. The sink is visible with dishes and utensils, indicating it's time to wash them. Turning off the sink tap is a necessary step to ensure the water doesn't run while washing dishes. Therefore, the next action should be to turn off the sink tap. </think>\n<answer>D</answer>

**APPO (Ours):** <think>The task at hand involves preparing bread, which typically includes washing hands before handling food to maintain hygiene. The first image shows the person is cooking on the stove and has just finished making something in a frying pan. After washing hands, the next logical step would be to dry them, which is a common practice after washing to prevent cross-contamination or to proceed with food preparation tasks. The subsequent images show the drying of hands, which aligns with the typical sequence of washing and drying hands before handling food. The options provided do not include drying hands, so the closest relevant action from the given choices would be to turn off the sink tap, as it is a necessary step before drying hands. However, since the question asks for the next action in the context of preparing bread, and considering the sequence of typical food preparation steps, the most logical next action after washing hands would be to dry them, which is not directly listed but implied by the sequence of actions. Therefore, the closest option to the logical next step in the context of the given choices is to turn off the sink tap, as it is a prerequisite for drying hands.</think>\n\n<answer>D</answer>

**Figure M** The visualization example from SEED-Bench-R1 Level-3 testset. The correct option is “D. turn off sink tap”. Our APPO algorithm successfully paid attention to the critical information of handwashing, which made subsequent logical reasoning more coherent.